

Revision 2

Sulfidation of native gold

Galina Palyanova^{1,2*}, Nicholas Karmanov¹, Natalie Savva³

¹*Sobolev Institute of Geology and Mineralogy, Siberian Branch of the RAS,*

²*Novosibirsk State University, Russian Federation*

³*North-East Interdisciplinary Scientific Research Institute, Far East Branch of the RAS*

Corresponding author:

Galina Palyanova

IGM SB RAS, Koptyuga ave., 3, Novosibirsk 630090, Russian Federation

*palyan@igm.nsc.ru,

ABSTRACT - We used microscopic and electron microprobe techniques to study samples of ores containing native gold with dark rims of Au-Ag sulfides from six deposits and ore occurrences of Russia: Khopto (Au-Cu-skarn), Ulakhan, Yunoe (Au-Ag epithermal), Dorozhnoe, Konechnoe and Yakutskoe (Au-quartz). Dark rims around native gold are uytenbogaardtite (Ag_3AuS_2) or petrovskaitite (AgAuS), or a mixture of acanthite (Ag_2S) with uytenbogaardtite or uytenbogaardtite with petrovskaitite. In the ore samples from the Khopto and Ulakhan deposits we have found microrims of higher fineness gold at the contact of native gold and Au-Ag sulfide. The reactions of native gold sulfidation occurring in natural processes are proposed based on the compositions of Au-Ag sulfides, their mutual textural relationships. The composition of Au-Ag sulfides rims was found to depend on the primary fineness of native Au: uytenbogaardtite after medium fineness gold (electrum) (>380‰) and petrovskaitite forms after high fineness gold (>650‰). We propose that the fineness of gold and silver may be used for forecasting presence of uytenbogaardtite or petrovskaitite, or a mixture of acanthite with uytenbogaardtite or uytenbogaardtite with petrovskaitite in the sulfide ores at Au-Ag epithermal, Au-skarn, Au-Cu volcanic-hosted massive sulfide, Au-quartz-sulfide and other deposits.

Keywords: uytenbogaardtite, petrovskaitite, native gold, fineness, reactions of sulfidation

INTRODUCTION

Gold and silver in nature occur in a native state, forming a continuous Ag-Au solid solution (White et al. 1957; Yushko-Zakharova et al 1986; Morrison et al. 1991; Pal'yanova 2008; Spiridonov and Yanakieva 2009). The fineness (N_{Au}) equal to $1000 \cdot \text{Au}/(\text{Au}+\text{Ag})$ (by weight) is used for the characterization of the composition of Au-Ag alloys or native gold and silver. Depending on the fineness (in ‰), the following native gold and silver are distinguished: "Au-

36 rich electrum" or "high fineness gold" (1000÷700), "electrum" (700÷250), "Ag-rich electrum" or
37 old term as "kustelite" (250÷100) and native silver (100÷0) (Boyle 1979; Petrovskaya 1993).
38 Silver nuggets are commonly covered with black crusts of silver sulfide - acanthite (Ag_2S). The
39 study of the chemical composition of dark rims on native gold has led to the discovery of the Au-
40 Ag sulfides - uytenbogaardtite (Ag_3AuS_2) (Barton et al. 1978) and petrovskaitite (AgAuS)
41 (Nesterenko et al. 1985). Mineral assemblages with these Au-Ag sulfides were found in Au-Ag
42 epithermal, Au-skarn, Au-Cu volcanogenic massive sulfide and Au-quartz-sulfide deposits
43 (Zhen-jie et al. 1979; Castor and Sjoberg 1993; Marcoux et al. 1993; Sheets et al. 1995; Dill
44 1998; Al'shevskii 2001; Greffie et al. 2002; Warmada et al. 2003; Chauvet et al. 2006; Koneev
45 2006; Majzlan 2009; Pal'yanova and Savva 2008; 2009; Anisimova et al. 2008; Proskurnin et al.
46 2011; Savva et al. 2012; Cocker et al. 2013). Au-Ag sulfides coexisting with native gold also
47 were stricken in the gold-placer mines of northeastern Russia (Al'shevskii 2001).

48 Au-Ag sulfides form veinlets, isolated microinclusions and 10-100 μm rims occurring in
49 native gold, rarely as single crystals and their aggregates 3-4 mm in size. Reaction rims are
50 formed when two phases or assemblages that cannot coexist stably are in contact and react to
51 produce a new phase or an assemblage along their interface (Fisher 1973). The specific chemical
52 mechanisms of reaction rim formation are not well understood for these systems. Numerous
53 disembodied data can be found in literature cited above on the fineness of native gold and
54 compositions of associated Au-Ag sulfides. The concentration of gold and silver in Au-Ag
55 sulfides, as well as in native gold, varies in a wide range (Savva and Pal'yanova 2007;
56 Pal'yanova 2008; Pal'yanova et al 2011). The objectives of the present study are to summarize
57 the available data on the sulfidation of native gold, to reveal compositional variations and
58 regularities and to explain the mechanism of Au-Ag sulfide formation. Uytenbogaardtite and
59 petrovskaitite are related to rare minerals which are not so widespread. However, the formation
60 mechanism of Au-Ag sulfides in natural conditions is important for understanding the
61 geochemistry, transport, and deposition of noble metals. Au-Ag sulfides were found in sulfide
62 ores of some deposits in amounts comparable to native gold, for example, Yunoe (Pal'yanova
63 and Savva 2009), Nazareno, Pongkor (Greffie et al 2002) and Broken Hills (Cocker et al. 2013),
64 and, therefore, their presence should be taken into account in the development of technological
65 schemes of Au and Ag concentration and recovery.

66

67 MATERIALS AND METHODS

68 We have thoroughly studied some polished sections of ore samples or mounts containing
69 grains of native gold with dark rims of Au-Ag sulfides from 6 deposits and ore occurrences of
70 Russia: Khopto (Au-Cu-skarn), Ulakhan, Yunoe (Au-Ag epithermal), Dorozhnoe, Konechnoe

71 and Yakutskoe (Au-quartz). Few grains of native gold with dark rims were found in concentrates
72 of ore minerals that remain after washing loose rocks (from Khopto and Dorozhnoe) with water
73 or dissolving the silicate matrix of dense ore samples (from Yunoe and Yakutskoe) with
74 hydrofluoric acid (Neuerburg, 1961) that allowed us to keep them from mechanical damage and
75 explore their surface. Before analysis, the surfaces of the polished sections and mounts were
76 thoroughly cleaned. Diagnostics of Au-Ag sulfides was performed using optical microscopy,
77 scanning electron microscopy (SEM) with energy-dispersive and wavelength-dispersive
78 spectrometers (WDS and EDS) and X-ray diffraction (XRD) methods.

79 The native gold, Au-Ag sulfides and other minerals were analyzed using JSM-6510LV SEM
80 (JEOL Ltd) combined with microanalysis system INCA Energy 350+ X-Max EDS (Oxford
81 Instruments) and MIRA 3 LMU SEM (TESCAN Ltd) combined with microanalysis system
82 INCA Energy 450+ on the basis of the high sensitive silicon drift detector XMax-80, and WDS
83 INCA Wave 500 (Oxford Instruments Ltd) (Novosibirsk, IGM SB RAS). The analyses were
84 conducted at 20 kV accelerating voltage and 1.5 nA probe current. Pure metals (Au and Ag), Au-
85 Ag alloys and pyrite (FeS₂) were used as the standards. Most analyses were performed using
86 SEM-EDS at 15-20 seconds live acquisition time of spectrum. Acquisition of spectra was
87 performed in the raster mode with the scanning area from 0.5x0.5 μm², for fine phases, and to
88 2x2 μm² for larger phases with a slightly defocused electron beam. This analysis mode reduces
89 the destructive effects of the electron beam on unstable Au-Ag sulfides. For analysis we used the
90 characteristic X-ray S K-series and L-series of Ag and Au. Under these conditions the random
91 error of measurement caused by the counting statistic for Au-Ag sulfide, corresponding to
92 uytenbogaardtite in composition, was 0.17, 0.37 and 0.98 wt % for S, Ag and Au, respectively.
93 Choice of Au L-series X-ray was due to the fact that in Au-Ag sulfides the spectra of S K-series
94 and Au M-series partially overlapped. The INCA Energy software permits deconvolution of
95 spectral lines but, due to the inaccurate accounting of the real lines shape, errors are possible. To
96 rule out this sort of mistakes, we carried out testing measurement of sulfur content on WDS and
97 EDS. The peak counting time S K_α was 60 sec, the background counting time was twice 30 sec,
98 live acquisition time of ED spectra was 85 sec. The standard deviation of counting statistic was
99 0.19 and 0.05 wt % for S (WDS and EDS), 0.17 and 0.51 wt % for Ag and Au (EDS). For
100 comparison we used the analyses the total of which lies in the range of 100±2 wt %. The
101 obtained testing data showed complete agreement of the results of WDS and EDS (n=20): S_{WDS}
102 – 12.23±0.45 wt %, S_{EDS} – 12.25±0.33 wt %, Ag – 31.77±1.42 wt %, Au – 55.43±1.49 wt %.

103 X-ray diffraction (XRD) analyses of some Au-Ag sulfides were carried out using DRON-4
104 (Cu K_α-radiation, Ni-filter) (Novosibirsk, IGM SB RAS) and Bruker D-8 Discovery equipment
105 (Cu K_α, graphite monochromator) (Novosibirsk, NSU). For the Debye-Scherrer camera

106 exposure, Au-Ag sulfides in the rims of polished sections were powdered under the microscope
107 using a diamond pyramid of microdrill, with the help of which an area of $20 \times 20 \mu\text{m}^2$ was
108 destroyed. The powder was put into a droplet of rubber which was glued to the quartz rod. The
109 X-ray studies showed that the Au-Ag sulfides are identical in characteristics to uytenbogaardtite
110 or petrovskaitite (sheets № 20-461 or 33-0587, 19-1146, JCPDS, 1999). Figure 1 shows the
111 diffraction pattern of Au-Ag sulfide from Khopto exhibiting characteristics to petrovskaitite (sheet
112 № 19-1146). Some weak peaks in the diffraction pattern can be interpreted as belonging to
113 uytenbogaardtite (sheet № 33-0587) and gold (sheet № 04-0784). X-ray study of Au-Ag-sulfides
114 from the Yakutskoe deposit was performed in (Nekrasov et al. 1988; Samusikov et al. 2002). For
115 the Au-Ag-sulfides from the Konechnoe deposit no XRD data were obtained because of the
116 small size of grains.

117 The composition of Au-Ag sulfides and native gold cited in literature was also obtained on
118 the basis of EDS and WDS-microprobe studies. Microprobe analysis of native gold and Au-Ag
119 sulfides revealed the presence of impurity elements such as Fe, Cu, Se and Te, but their content
120 was less than 1 wt %, and in most cases even less than 0.5 wt % (Castor and Sjoberg 1993;
121 Marcoux et al. 1993; Sheets et al. 1995; Greffie et al. 2002; Warmada et al. 2003; Majzlan
122 2009).

123

124 **RESULTS**

125 The grain of native gold with a dark rim of Au-Ag sulfide from the Khopto deposit is shown
126 in Figure 2a,b. Fig. 2 c-g illustrates a representative energy-dispersive (ED) spectra of
127 petrovskaitite (c) and native gold of fineness 820-880 ‰ (d) as well as the distribution of Ag (e),
128 Au (f) and S (g) on the scanning area in characteristic rays. The considerable variations of Ag
129 and Au concentrations in Au-Ag sulfide were established with the S concentration varying in a
130 narrower range (Table 1). This mineral has an intermediate composition between
131 uytenbogaardtite and petrovskaitite, as it is enriched in S and Ag and is depleted in Au compared
132 to the ideal composition of petrovskaitite. It is also enriched in S and Au and is depleted in Ag
133 compared to ideal composition of uytenbogaardtite. Previously, the higher Ag concentrations and
134 lower Au concentrations established for a Au-Ag sulfide from the Khopto deposit were assigned
135 to uytenbogaardtite (Gas'kov et al. 2006).

136 However, a higher resolution study of the grains of native gold with dark rims from the
137 Khopto deposit under the MIRA 3 LMU SEM at magnifications of about $\times 70000$ - 10000 showed
138 that they consists of several phases (Fig. 3). One of the minerals (3-5 μm thick) (Fig. 3a, grey) is
139 close to petrovskaitite (Fig. 3d), whereas another one (Fig. 3a, dark-grey) is Ag-enriched and Au-
140 depleted and is close to uytenbogaardtite (Fig. 3c) (Table 1). In addition, there is a microrim of

141 higher fineness gold (930‰) on the contact between native gold (820‰) and Au-Ag sulfides
142 (Fig. 3a,e,f). Backscattered electron images (BSE) reveal that, when in contact with petrovskaitite,
143 native gold has a higher Au content producing a brighter zone in the BSE (Fig. 3a). Line scans of
144 the contact zone between native gold and Au-Ag sulfides show changes in the Au, Ag, and S
145 contents, with Au-rich areas near grain boundaries with petrovskaitite (Fig. 3b).

146 Similar to previous observations (Savva and Pal'yanova 2007) we also found microrims of
147 higher fineness gold (660 - 720‰) on the contact between Au-Ag sulfides and native gold of
148 fineness 350 - 370 ‰ in the Ulakhan samples (Fig. 4). Native gold in the rim has a higher Au
149 content producing a brighter zone in the BSE (Fig. 4b-d). Au-Ag sulfides are intimately
150 intergrown with each other (dark-grey and grey phases) and with Au of higher fineness (Fig.
151 4c,d). The dark-grey phase corresponds to acanthite, and the grey phase is uytenbogaardtite
152 (Table1). Both phases are characterized by high S contents as compared to the Ag_2S and
153 Ag_3AuS_2 stoichiometric composition.

154 Detailed analysis of samples from the Yakutskoe deposit showed the absence of high
155 fineness gold micro rim on the contact between petrovskaitite and native gold (Fig.5a-c). Native
156 gold has a fineness of 650 - 680 ‰, and the composition of Au-Ag sulfide corresponds to
157 petrovskaitite with lower Ag contents and higher Au and S contents (Table1). Figure 5d shows the
158 concentrations of Au, Ag and S in the points of scanning in the section across native gold and
159 Au-Ag sulfide. The variations of Au and Ag in native gold and those of Au, Ag and S in
160 petrovskaitite are minor. The compositions of native gold and petrovskaitite compositions from the
161 Yakutskoe deposit in our study agree well with earlier data (Nekrasov et al. 1988). Study of
162 intermediate micro rims with Au of high fineness was not found on the contact between native
163 gold with rims of Au-Ag sulfides (Table1) from the Yunoe, Dorozhnoe and Konechnoe deposits.

164 We analyzed the composition of native gold and Au-Ag sulfides and identified types of
165 intergrowths of these minerals based on previously published data and our analysis. The five
166 types of sulfide intergrowths associated with the fineness of native gold at the contact with Au-
167 Ag sulfides for some deposits were summarized in Table 2. We distinguish the occurrences of
168 Au as “primary” (generation I) and “secondary” gold (generation II). “Secondary” gold is
169 present between Au-Ag sulfide and primary gold, and corresponds to late stage Au
170 mineralization after sulfidation. In some cases, the higher fineness native gold is also considered
171 secondary (later gold) relative to early generation gold (Castor and Sjöberg 1993; Greffie et al.
172 2002; Cocker et al. 2013).

173 The first type of intergrowths (1) is characterized by a sharp contact of one of the Au-Ag
174 sulfides (acanthite, uytenbogaardtite or petrovskaitite) with native gold. The petrovskaitite rims
175 around native gold, shown in Fig. 5a-c, are an example of type 1 intergrowths. Dark rims in type

176 2 are represented by thin intergrowths of two Au-Ag sulfides - acanthite with uytenbogaardtite or
177 uytenbogaardtite with petrovskaitite around the grains of native gold. This type is very common
178 and typical of many deposits (Table 2). Types 3 and 4 differ from types 1 and 2 with high
179 fineness Au (II) micro rims in contact with native primary gold (I) and sole Au-Ag sulfide or two
180 Au-Ag sulfides, respectively. The third type of intergrowth relationships is typical of Lac and
181 Original Bullfrog, Nazareno and Broken Hills (Table 2). Sharp contacts between native gold I, II
182 and Au-Ag sulfides (acanthite and uytenbogaardtite or uytenbogaardtite and petrovskaitite) (type
183 4) are described for the Ulakhan (Fig. 4), Khopto (Fig. 3a), Nazareno, Pongkor and other
184 deposits (Table 2). Barton et al. (1978) and Greffie et al. (2002) showed the 5-th type of
185 intergrowths, when acanthite is replaced by uytenbogaardtite followed by rims of native gold II
186 and I. It is typical of the Comstock and Pongkor deposits (Table 2).

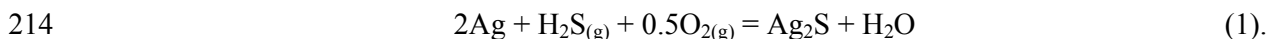
187 The summary on the chemical composition of acanthite, uytenbogaardtite and petrovskaitite at
188 the contact with native gold and silver in the mutual intergrowths suggests that the composition
189 of the Au-Ag sulfides and fineness of secondary gold depends on the fineness of the primary
190 gold. Native silver and Ag-rich electrum (0-250 ‰) is replaced by acanthite (Comstock and
191 others), native gold of fineness 350-520 ‰ by uytenbogaardtite (Konechnoe) and high fineness
192 gold (above 650 ‰) by petrovskaitite (Yakutskoe and others) (Table 2, type 1). The native gold of
193 fineness 360-700 ‰ is replaced by a mixture of acanthite with uytenbogaardtite (Tambang
194 Sawah and others). The native gold of fineness 870-880 ‰ is surrounded by a mixture of
195 uytenbogaardtite with petrovskaitite (Dorozhnoe, Krutoe) (Table 2, type 1). It is established that
196 the fineness of native gold II in the intermediate micro rims is higher than the fineness of
197 primary gold (Table 2, types 3 and 4). So, the native gold in the rims between uytenbogaardtite
198 and the native gold I (560-740 ‰) has higher fineness (700-870 ‰) at the Lac Bullfrog and
199 others. The central part of the native Au grains is enriched in silver (450 ‰) compared to the
200 intermediate micro rim (600 ‰) located at the contact with uytenbogaardtite around native
201 primary gold and enclosed by acanthite at the Comstock deposit (type 5) (Barton et al. 1978).

202 The triangular diagram of the Ag-Au-S system (Fig. 6a,b) demonstrates that the Ag/Au
203 proportion in primary gold and Au-Ag sulfides is regularly higher than secondary gold for the
204 Khopto and Ulakhan deposits (type 4). Fig. 6c shows that the Au/Ag proportion in Au-Ag
205 sulfides and native Au of Yakutskoe deposit is identical (type 1). The data presented in triangular
206 and binary diagrams, showing the compositions of Ag-Au-S-minerals for other deposits (Barton
207 et al. 1978; Greffie et al. 2002; Cocker et al. 2013), confirm that the composition of the Au-Ag
208 sulfides and fineness of secondary gold depends on the fineness of primary gold.

209

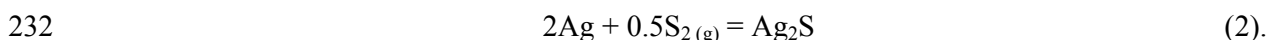
210 **DISCUSSION**

211 It is well known that silver is not stable in the presence of hydrogen sulfide ($\text{H}_2\text{S}_{(g)}$) and other
212 sulfide phases even in small abundances. Under the effect of $\text{H}_2\text{S}_{(g)}$ on metal silver in the
213 presence of atmospheric oxygen Ag_2S forms by the following reaction:

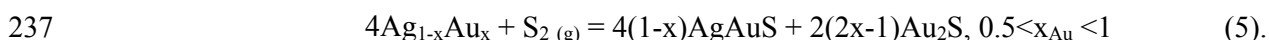
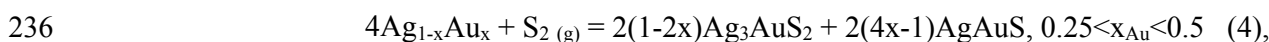
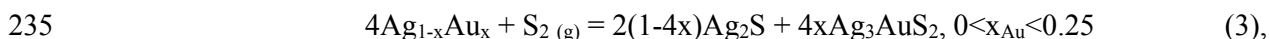


215 The appearance of a dark rims on native gold are also attributed to Ag_2S (Meretukov 2008).
216 Here, however, we also show that tarnishing of the native gold is related not only to the
217 occurrence of silver sulfide Ag_2S , but also to Ag_3AuS_2 and AgAuS sulfides.

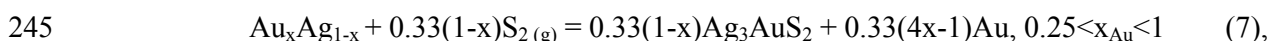
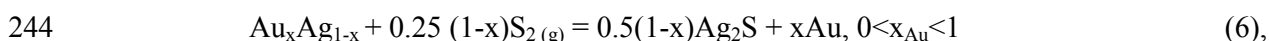
218 Reactions involving sulfides are controlled by the chemical potentials of sulfur or S-bearing
219 components in the environment in which they occur. In geologic environments, S exists in liquid
220 (l), solid (s) and volatile (g) phases (Simon and Ripley 2011). Sulfur in the solid state is found as
221 native S and as the base for all sulfide and sulfate minerals. Elemental S (l or s) is abundant near
222 hot springs, in volcanic fumaroles, in salt domes, and in evaporates. Sulfur in the gaseous state
223 exists dominantly as $\text{H}_2\text{S}_{(g)}$ and $\text{SO}_{2(g)}$. Common oxidation states in near-surface geologic
224 reservoirs include S^0 , S^{2-} , and S^{6+} , where S is bonded with oxygen as sulfate SO_4^{2-} . The
225 chemical potential of sulfur in geologic systems is represented by the use of the fugacity of
226 sulfur ($f\text{S}_2$) (Garrels and Christ 1965). Formation of sulfide mineral assemblages in the current
227 models of ore deposits genesis are usually solid-phase reactions involving gaseous sulfur
228 (Sillitoe and Hedenquist 2003; Einaudi et al 2003; Simon and Ripley 2011 and other). For
229 example, Barton and Toulmin (1964) express the formation of Ag_2S in laboratory experiments
230 under the effect of $\text{S}_{2(g)}$ on metal silver in the absence of other S-bearing components by the
231 following reaction:

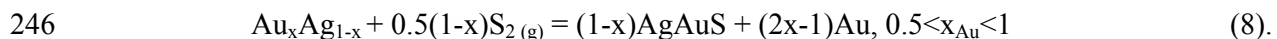


233 Sulfidation reactions of native gold or alloy $\text{Au}_x\text{Ag}_{1-x}$ ($0 < x < 1$, where x - atomic fraction of gold)
234 with $\text{S}_{2(g)}$ may take place along with the precipitation of Au-Ag sulfides (Fig. 7a):

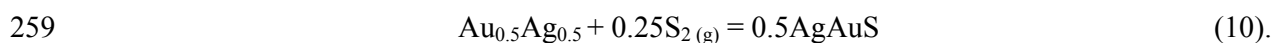
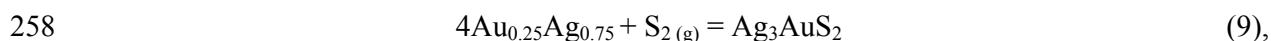


238 These reactions were also proposed by Gurevich et al. (2011), when interpreting experimental
239 data in the system Ag-Au-S. Reactions 3 and 4 explain the formation of two Au-Ag sulfides
240 simultaneously, but do not explain the formation of intermediate microfilm of higher fineness
241 gold observed in some natural samples. We suggest, therefore, that metastable formation of
242 Ag_2S , Ag_3AuS_2 or AgAuS and secondary Au of high fineness are more applicable to natural
243 processes (Fig. 7b):





247 Changes in the composition of native gold and coexisting mineral assemblages are schematically
248 shown in the ternary Ag-Au-S composition diagram (Fig.7a,b). The formation of AgAuS
249 (reaction 8) or AgAuS with Ag₃AuS₂ (reaction 4) can occur at 0.5 < x_{Au} < 1, when the fineness of
250 primary Au-Ag alloy is 650 – 999 ‰. Precipitation of Ag₃AuS₂ (reaction 7) and Ag₃AuS₂ with
251 Ag₂S (reaction 3) is possible at 0.25 < x_{Au} < 0.5, when the fineness of primary Au-Ag alloy is 380 –
252 650 ‰. Reaction 5 is theoretically feasible when x_{Au} < 1. Ag₂S forms at x_{Au} < 0.25 along with
253 Ag₃AuS₂ and AgAuS. When x_{Au} equal 0.25 or 0.5 (primary Au of 380 or 650 ‰ fineness),
254 reactions 7 and 8 become identical 3 and 4, because the molar ratio Ag/Au in the initial native
255 gold (0.75/0.25 = 3/1 or 0.5/0.5=1/1) corresponds to the molar ratio of Ag/Au in
256 uytenbogaardtite (3/1) or petrovskaitite (1/1). Reactions 7 and 8 proceed without formation of
257 secondary gold, and reactions 3 and 4 form only one Au-Ag sulfide (Ag₃AuS₂ or AgAuS):



260 Reactions of sulfidation in the Ag-Au-S system depend on temperature and sulfur fugacity
261 (Barton et al. 1978; Barton 1980; Gurevich et al. 2011). Phase equilibrium constraints on a log
262 $f\text{S}_2 - 1 / T$ diagram suggest that uytenbogaardtite and petrovskaitite occur at very high sulfur
263 fugacity near the phase boundary of S₍₁₎-S_(g) [Barton et al. 1978; Barton 1980]. However,
264 Gurevich et al. (2011) calculated the univariant reactions 2, 9 and 10 and concluded that
265 equilibria involving petrovskaitite and uytenbogaardtite do not necessarily require such elevated
266 sulfur fugacity. As for reaction 5, it does not occur in natural processes since gold sulfide is
267 metastable at ambient conditions (Barton 1980; Renders and Seward 1989). Au₂S decomposed
268 into Au and S under inert atmosphere or Au and SO_{2(g)} over 217°C and atmospheric conditions
269 (Ishikawa et al. 1995). A thermodynamic model for “invisible gold” as a tri-atomic surface
270 complex Au₂S or AuS₂ dispersed in the crystalline structure of the pyrite (FeS₂) and arsenopyrite
271 (FeAsS) has also been developed (Yang et al. 1998; Simon et al. 1999). Gold sulfide is not
272 formed even when the gold reacts with liquid sulfur or under conditions of elevated temperature
273 and sulfur fugacity (Barton and Toulmin 1964; Pal’yanova et al 2011).

274 The formation of rims with uytenbogaardtite (Konechnoe) or petrovskaitite (Yakutskoe,
275 Maikain, Broken Hills) (Table 2, type 1) is most likely the result of reactions 9 and 10 (Fig.7a,b),
276 when the composition of native gold is close or equal to x_{Au} ≈ = 0.25 and 0.5, corresponding to
277 the fineness 380 and 650 ‰. Type 2 intergrowths, which include mixture of Au-Ag sulfides with
278 native gold (see Table 2), are formed by reactions 3 or 4 (Fig.7a). Formation of type 3
279 intergrowths with a microrim of higher fineness gold II between uytenbogaardtite and Au I (the

280 Lac Bullfrog, Original Bullfrog, Nazareno, Broken Hills) (Table 2) most likely is attributed to
281 the reaction 7 (Fig.7b).

282 The rims of type 4 formed during the sulfidation of native gold in the Morning Star,
283 Nazareno, Cirotan, Ulakhan and Broken Hills deposits (Table 1), are explained by the reactions 3
284 and 7 (Fig.7a,b). The rims of 4 type formed during the sulfidation of native gold at the Khopto
285 are apparently the result of reactions 4 and 8. Type 5 of intergrowths are explained by the
286 reactions 6 and 7 (Fig.7b).

287 Extraction of silver from Au-Ag alloy to form acanthite or uytenbogaardtite or petrovskaitite
288 would cause an increase in gold fineness. As the result of disequilibrium processes during
289 sulfidation, a rim with higher fineness secondary gold II is formed between primary native gold I
290 and Au-Ag sulfides by reactions 6-8 (Fig.7b). During sulfidation of native gold the appearance
291 of Au-Ag sulfide can be accompanied by the formation of higher fineness gold, because the
292 enrichment with gold takes place at the expense of silver spent on the formation of Ag_3AuS_2 or
293 $AgAuS$. The corrosion-disordering/diffusion-reordering mechanism of enrichment of the surface
294 of low fineness Au-Ag alloys due to the removal of silver is described by Rapson (1996). The
295 dissolution of Ag atoms and inward migration of the vacancies is the result of the action of
296 different reagents. High fineness rims are typical placer of native gold (Craig and Vaughan 1981;
297 Petrovskaya 1993). Silver is more mobile and is carried out from the surface layer by meteoric
298 waters (Savva and Pal'yanova 2007; Savva et al. 2010).

299 Thus, Au-Ag sulfides form in a wide temperature range in the presence of S-containing
300 compounds. Reactions 1-10 are oversimplified with respect to natural reactions and can be
301 changed by any S-containing compounds. Which of the reactions is realized, depends on the
302 primary fineness of native gold and the sulfur forms of occurrence. The composition of Au-rich
303 microrims will depend on the fineness of primary gold.

304 We analyzed the surface of native gold grains from the oxidation zone of the Dorozhnoe
305 deposit. The grains of native gold were partially covered with dark rims of Au-Ag sulfide. Figure
306 8 shows the porous structure of high fineness native gold (a) and the presence of Au-Ag sulfide
307 microcrystals (b). These data show a more intensive removal of silver and redeposition of noble
308 metals in the form of Au-Ag sulphide. Uytenbogaardtite and petrovskaitite at the Dorozhnoe
309 deposit have a hypogene genesis, like at the Ulakhan and the Krutoe deposits (Savva and
310 Palyanova 2007; Pal'yanova and Savva 2008; Savva et al. 2010).

311 The obtained results and available published data show that conditions of metastable
312 equilibria play a significant role in the formation of uytenbogaardtite and petrovskaitite. The
313 replacement of one mineral by another encompasses most processes of nonequilibrium.

314 The probable genesis of uytenbogaardtite and petrovskaitite was discussed in a number of
315 studies (Barton 1980; Castor and Sjöberg 1993; Marcoux et al. 1993; Sheets et al. 1995; Dill
316 1998; Al'shevskii 2001; Greffie et al. 2002; Warmada et al. 2003; Chauvet et al. 2006; Majzlan
317 2009; Pal'yanova and Savva 2008; 2009; Savva et al. 2012; Pal'yanova et al. 2012; Cocker et al.
318 2013 and other). Depending on the composition of mineral associations and their formation
319 conditions, Au-Ag sulfides can be both of hypogene and hypergene origin. At the majority of
320 deposits (for example, Ulakhan, Krutoe, Nazareno, Pongkor) they were found in the zone of
321 oxidation together with acanthite, high fineness gold and hypergene minerals such as ferric
322 hydroxide, jarosite, melanterite, malachite, azurite, chrysocolla, covellite, scorodite, pyrolusite,
323 and manganite. We suggest that the formation of Au-Ag sulfides in these deposits corresponds to
324 sulfidation of primary native gold and during oxidation of pyrite or other sulfides (galenite,
325 sphalerite, and acanthite) by natural surface waters. In other ore deposits (for example, Cirotan,
326 Yunoe, and other) Au-Ag sulfides were found in mineral hypogene parageneses. These minerals
327 can form in high-temperature hydrothermal solutions enriched in H_2S_{aq} . Sulfidation reactions of
328 earlier deposited native gold driven by S-bearing volcanic gases (H_2S_g , SO_{2g}) or by H_2SO_4 -rich
329 hydrothermal-meteoric waters have been suggested as a plausible mechanism for the formation
330 of Au-Ag sulfides at the Kupol deposit (Savva et al 2012).

331 The mechanism of native gold formation from volcanic gases has been confirmed by many
332 researchers (Symonds et al. 1990; Korzhinskii et al. 1996; Vergasova et al. 2000). Native gold
333 and silver were found in fumaroles' fields of Russian (Kamchatka) and Mexican volcanoes
334 (Naboko and Glavatskikh 1996; Taran et al. 2000). The presence of modern sulfurous fumaroles
335 on the walls of craters and thermal H_2SO_4 -rich lakes (Giggenbach 1987; Pasternack and
336 Varekamp 1997) in craters suggests that Au-Ag sulfides can be formed at epithermal deposits
337 during solfatara and postsolfatara processes (Savva et al 2012). At temperatures of 113-1040°C
338 ($T_{melt} - T_{critical}$) sulfur may not only be as gas but also as liquid phase. Liquid sulfur is
339 characterized by high reactivity (Malyshev 2004), favoring the kinetics of these reactions. Such a
340 mechanism can be realized in a metamorphic process, when under the influence of temperature
341 and pressure native sulfur melts and interacts with the early native gold.

342 Uytenbogaardtite and petrovskaitite were also stricken in magmatic rocks and ores. For
343 example, Au-Ag sulfides of $(Au,Ag,Fe)_2S$ composition were found together with the sulfides of
344 iron, copper and nickel in carbon-bearing chondrites (Geiger and Bischoff 1995).
345 Uytenbogaardtite in association with electrum has been found in ijolite and nepheline syenites
346 from the Goryachegorskii massif (Sazonov et al. 2008).

347 Barton (1980) introduced corrections into the evaluation of sulfur fugacity by electrum-
348 tarnish method developed by Barton and Toulmin (1964). Only acanthite was taken into account,

349 because the fineness of Au-Ag alloys in association with uytenbogaardtite was higher than 890
350 ‰ ($x_{Au}>0.82$) and petrovskaitite was higher than 940 ‰ ($x_{Au}>0.9$), according to experimental and
351 calculated results. In all natural assemblages the native gold is Ag richer than was predicted for
352 the three phase assemblages acanthite-electrum-uytenbogaardtite and uytenbogaardtite-electrum-
353 petrovskaitite. The results obtained in our work indicate the need for further adjustments to the
354 method of tarnishing electrum in applying it to natural processes and taking into account of non-
355 equilibrium and the variety of ore-forming environments.

356

357 **IMPLICATIONS**

358 Dark rims on native gold are related to the presence of Au-Ag sulfides – acanthite (Ag_2S),
359 uytenbogaardtite (Ag_3AuS_2), petrovskaitite ($AgAuS$) or their mixtures - acanthite with
360 uytenbogaardtite or uytenbogaardtite with petrovskaitite. Sulfidation of native gold occurs through
361 the chain of local equilibria involving phases Ag_2S , Ag_3AuS_2 , $AgAuS$ and a secondary high
362 fineness gold. The composition of dark films depends on the fineness of native gold: petrovskaitite
363 forms after high fineness gold ($>650\%$) and uytenbogaardtite after medium fineness gold
364 (electrum $>380\%$).

365 The revealed dependence of composition of Au-Ag sulfides on native gold fineness has
366 implications for the treatment of gold-sulfide ores and for understanding the origin of some
367 unusual assemblages in nature. From the fineness of native gold one can forecast the
368 composition of associated Au-Ag sulfide(s). The established main regularities of sulfidation of
369 native gold may also take place in artificial Au-Ag alloys. Our estimations show that a rim of
370 $AgAuS$ composition forms after 18 carat gold (750 ‰), Ag_3AuS_2 develops after 14 – 9 carat
371 alloys (583-375 ‰), whereas Ag_2S forms after low fineness alloys and silver.

372

373 **ACKNOWLEDGEMENTS**

374 The reported study was supported by RFBR (research project №11-05-00504a), SB and FEB RAS
375 (Integration project № 12 and 48). We would like to express our sincere thanks to the editor and
376 anonymous reviewers for their comments and constructive suggestions improving the quality of this
377 manuscript. Special thanks to one of the reviewers for correcting the English language of the manuscript.
378 We thank Yu. V. Seryotkin and V.S. Pavlyuchenko (IGM SB RAS) for the data of XRD study.

379

380 **REFERENCES**

- 381 Al'shevskii, A.V. (2001) Gold sulfide minerals in northeastern Russia: occurrence, composition,
382 and genesis, In *The Problems of Geology and Metallogeny in Northeastern Russia at the*
383 *Boundary of the Millennia*, 2, 135–138, North-East Interdisciplinary Scientific Research
384 Institute, Far East Branch, Russian Academy of Sciences, Magadan (in Russian).
385 Anisimova, G.S., Kondrat'eva, L.A., and Leskova, N.V. (2008) Gold and silver compounds in
386 gold deposits in Eastern Yakutia. *Otechestvennaya Geologiya*, 5, 24–32 (in Russian).
387 Archibald, S.M., Migdisov, A.A. and Williams-Jones, A.E. (2001) The stability of Au-chloride
388 complexes in water vapor at elevated temperatures and pressures. *Geochimica et*
389 *Cosmochimica Acta*, 65, 4413–4423.

- 390 Barton, M.D. (1980) The Ag-Au-S system. *Economic Geology*, 75, 303–316.
- 391 Barton, M.D., Kieft, C., Burke, E.A.J. and Oen, I.S. (1978) Uytendogaardite, a new silver–gold
392 sulfide. *Canadian Mineralogist*, 16, 651–657.
- 393 Barton, P.B. and Toulmin, P. (1964) The electrom-tarnish method for the determination of the
394 fugacity of sulfur in laboratory sulfide systems. *Geochimica et Cosmochimica Acta*, 28,
395 619–640.
- 396 Boyle, R.W. (1979) *The Geochemistry of Gold and Its Deposits*. Geol. Surv. Canada, Ottawa.
- 397 Castor, S.B. and Sjöberg, J.J. (1993) Uytendogaardite, Ag₃AuS₂, in the Bullfrog mining district,
398 Nevada. *Canadian Mineralogist*, 31, 89–98.
- 399 Chauvet, A., Bailly, L., André, A.-S., Monié, P., Cassard, D., Tajada, F.L., Vargas, J.R. and
400 Tuduri, J. (2006) Internal vein texture and vein evolution of the epithermal Shila-Paula
401 district, southern Peru. *Mineralium Deposita*, 41, 387–410.
- 402 Cocker, H.A., Mauk, J.L. and Rabone, S.D.C. (2013) The origin of Ag-Au-S-Se minerals in
403 adularia-sericite epithermal deposits: constraints from the Broken Hills deposit, Hauraki
404 Goldfield, New Zealand. *Mineralium Deposita*, 48, 249–266.
- 405 Craig, J.R. and Vaughan, D.J. (1981) *Ore microscopy and ore petrography*. Chichester and New
406 York (John Wiley and Sons Ltd: Wiley-Interscience).
- 407 Dill, H.G. (1998). Evolution of Sb mineralisation in modern fold belts: a comparison of the Sb
408 mineralisation in the Central Andes (Bolivia) and the Western Carpathians (Slovakia).
409 *Mineralium Deposita*, 33, 359–378.
- 410 Einaudi, M.T., Hedenquist, J.W. and Inan, E.E. (2003) Sulfidation state of fluids in active and
411 extinct hydrothermal systems: Transitions from porphyry to epithermal environments.
412 *Society of Economic Geologists Special Publication*, 10, 285–313.
- 413 Fisher, G.W. (1973) Nonequilibrium thermodynamics as a model for diffusion-controlled
414 metamorphic processes. *American Journal of Science*, 273, 897–924.
- 415 Gammons, C.H. and Williams-Jones, A.E. (1995) Hydrothermal geochemistry of electrum:
416 thermodynamic constraints. *Economic Geology*, 90, 420–432.
- 417 Garrels, R.M. and Christ, C.L. (1965) *Solutions, minerals and equilibria*, 450p. Harper and Row,
418 New York.
- 419 Gas'kov, I.V., Akimtsev, V.A., Kovalev, K.R. and Sotnikov, V.I. (2006) Gold-bearing mineral
420 assemblages of Cu-ore deposits in the Altai-Sayan folded area. *Russian Geology and*
421 *Geophysics*, 47, 996–1004.
- 422 Geiger, T. and Bischoff, A. (1995) Formation of opaque minerals in CK chondrites. *Planetary*
423 *Space Science*, 43 (3–4), 485–498.
- 424 Giggenbach, W.F. (1987) Redox processes governing the chemistry of fumarolic gas discharges
425 from White Island, New Zealand. *Applied Geochemistry*, 2 (2), 143–161.
- 426 Greffie, C., Bailly, L. and Milesi, J.-P. (2002) Supergene alteration of primary ore assemblages
427 from low-sulfidation Au-Ag epithermal deposits at Pongkor, Indonesia, and Nazareno,
428 Peru. *Economic Geology*, 97, 561–571.
- 429 Gurevich, V. M., Gavrichev, K. S., Osadchii, E. G., Tyurin, A.V. and Ryumin, M. A. (2011)
430 Heat Capacity and Thermodynamic Functions of Petrovskaita (AgAuS) at 0–583 K and
431 Mineral Equilibria in the Ag–Au–S System. *Geochemistry International*, 49, 422–428.
- 432 Ishikawa, K., Isonaga, T., Wakita, S. and Suzuki, Y. (1995) Structure and electrical properties of
433 Au₂S. *Solid State Ionics*, 79, 60–66.
- 434 Knacke, O., Kubaschewski, O. and Hesselmann, K. (1991) *Thermochemical properties of*
435 *inorganic substances*. Berlin, Heidelberg, Springer-Verlag.
- 436 Koneev, R.I. (2006) Nanomineralogy of gold, 220 p. Delta, St. Petersburg (in Russian).
- 437 Korzhinskii, M.A., Tkachenko, S.I., Bulgakov, R.F. and Shmulovich, K.I. (1996) Compositions
438 of condensates and native metals in sublimates of high-temperature gas jets of Kudryavyy
439 Volcano, Iturup Island (Kurile Isles). *Geokhimiya*, 12, 1175–1182.
- 440 Majzlan, J. (2009) Ore mineralization at the Rabenstein occurrence near Banská Hôrka,
441 Slovakia. *Mineralia Slovaca*, 41, 45–54.

- 442 Malyshev, A.I. (2004) Sulfur in magmatic ore formation, 190p. IGG UrO RAN, Yekaterinburg
443 (in Russian).
- 444 Marcoux, E., Milesi, J.P., Sonearto, S. and Rinawan, R. (1993) Noteworthy Mineralogy of the
445 Au–Ag–Sn–W(Bi) Epithermal Ore Deposit of Cirotan, West Java, Indonesia. Canadian
446 Mineralogist, 31, 727–744.
- 447 Meretukov, M.A. (2008) Gold: chemistry, mineralogy, and metallurgy, 528 p. Ruda i Metals,
448 Moscow (in Russian).
- 449 Migdisov, A.A., Williams-Jones, A.E. and Suleimenov, O.M. (1999) Solubility of chlorargyrite
450 (AgCl) in water vapor at elevated temperatures and pressures. Geochimica et
451 Cosmochimica Acta 63, 3817–3827.
- 452 Morrison G.W., Rose W.J. and Jareith S. (1991) Geological and geochemical controls on the
453 silver content (fineness) of gold in gold-silver deposits. Ore Geology Reviews, 6, 333-
454 364.
- 455 Naboko, S.I. and Glavatskikh, S.F. (1996) Gold and silver in volcanogenic fluid regime.
456 Vulkanologiya i Seismologiya, 6, 3–19 (in Russian).
- 457 Nekrasov, I.Ya., Samusikov, V.P. and Leskova, N.V. (1988) The first finding of AgAuS, a
458 petrovskaita analog. Doklady Earth Sciences, 303 (4), 944–947 (in Russian).
- 459 Nesterenko, G.V., Kuznetsova, A.I., Palchik, N.A. and Lavrentev, Yu.G. (1985) Petrovskaita.
460 American Mineralogist, 70, 1329.
- 461 Neuerburg, G.J. (1961) A method of mineral separation using hydrofluoric acid. American
462 Mineralogist, 46, 1498-1501.
- 463 Osadchii, E.G. and Rappo, O.A. (2004) Determination of standard thermodynamic properties of
464 sulfides in the Ag-Au-S system by means of a solid-state galvanic cell. American
465 Mineralogist, 89, 1405–1410.
- 466 Pal'yanova, G. (2008) Physicochemical modeling of the coupled behavior of gold and silver in
467 hydrothermal processes: gold fineness, Au/Ag ratios and their possible implications.
468 Chemical Geology, 255, 399–413.
- 469 Pal'yanova, G.A. and Savva, N.E. (2008) Some sulfides of gold and silver: composition, mineral
470 assemblage, and conditions of formation. Theoretical Foundations of Chemical
471 Engineering, 42, 749–761.
- 472 Pal'yanova, G.A. and Savva, N.E. (2009) Specific genesis of gold and silver sulfides at the
473 Yunoe deposit (Magadan Region, Russia). Russian Geology and Geophysics, 50, 579-
474 594.
- 475 Pal'yanova, G.A., Kokh, K.A. and Seryotkin, Yu.V. (2011) Formation of gold and silver sulfides
476 in the system Ag-Au-S. Russian Geology and Geophysics, 52, 443-449.
- 477 Pal'yanova, G.A., Kokh, K.A. and Seryotkin, Yu.V. (2012) Formation of gold–silver sulfides
478 and native gold in Fe–Ag–Au–S system. Russian Geology and Geophysics, 53, 347-355.
- 479 Pasternack, G.B. and Varekamp, J.C. (1997) Volcanic lake systematics. I. Physical constraints.
480 Bulletin of Volcanology, 58, 528-538.
- 481 Petrovskaya, N.V. (1993) Gold nuggets. Nauka, Moscow (in Russian).
- 482 Proskurnin, V.F., Pal'yanova, G.A., Karmanov, N.S., Bagaeva, A.A., Gavrish, A.V. and
483 Petrushkov, B.S. (2011) The first discovery of uytenbogaardtite in Taimyr (Konechnoe
484 ore occurrence). Doklady Earth Sciences, 441, 1661–1665.
- 485 Rapson, W.S. (1996) Tarnish resistance, corrosion and stress corrosion cracking of gold alloys.
486 Gold Bulletin, 29, 61-69.
- 487 Renders, P.J. and Seward, T.M. (1989) The stability of hydrosulphido- and sulphido-complexes
488 of Au(I) and Ag(I) at 25 °C. Geochimica et Cosmochimica Acta, 53, 245–253.
- 489 Samusikov, V.P., Nekrasov, I.Ya. and Leskova, N.V. (2002) Gold-silver sulfoselenide
490 (AgAu)₂(S,Se) from the Yakutskoe deposit. Zapiski Vsesousnogo Mineralogicheskogo
491 Obshchestva, 6, 61–64 (in Russian).
- 492 Savva, N.E., and Pal'yanova, G.A. (2007) Genesis of gold and silver sulfides at the Ulakhan
493 deposit (northeastern Russia). Russian Geology and Geophysics, 48, 799-810.

- 494 Savva, N.E., Pal'yanova, G.A. and Kolova, E.E. (2010) Gold and silver minerals in zone of
495 secondary sulfide enrichment (Krutoe ore occurrence, northeastern Russia). Bulletin of
496 the North-East Scientific Center, Russian Academy of Sciences Far East Branch, 1, 33–
497 45 (in Russian).
- 498 Savva, N.E., Pal'yanova, G.A., and Byankin, M.A. (2012) The problem of genesis of gold and
499 silver sulfides and selenides in the Kupol deposit (Chukot Peninsula, Russia). Russian
500 Geology and Geophysics, 53, 457-466.
- 501 Sazonov, A.M., Zvyagina, E.A., Leontiev S.I., Wolf, M.V., Poleva T.V., Chekushin V.S. and
502 Oleinikova N.V. (2008) Associations of micro- and nano- sized aggregates of precious
503 metals in ores. Journal of Siberian Federal University: Engineering & Technologies,
504 1,17-32. (in Russian)
- 505 Selected Powder Diffraction Data for Education and Training. (1999) Search Manual and Data
506 Cards, JCPDS, ICDD, Pennsylvania, USA.
- 507 Sheets, R.W., Craig, J.R. and Bodnar, R.J. (1995) Composition and occurrence of electrum at the
508 Morning Star deposit, San Bernardino County, California evidence for remobilization of
509 gold and silver. Canadian Mineralogist, 33, 137–151.
- 510 Sillitoe, R.H. and Hedenquist, J.W. (2003) Linkages between volcanotectonic settings, ore-fluid
511 compositions, and epithermal precious metal deposits, in Society of Economic
512 Geologists. Special Publication, 10, 315-343.
- 513 Simon, A.C. and Ripley, E.M. (2011) The role of magmatic sulfur in the formation of ore
514 deposits. In: Sulfur in magmas and melts: Its importance for natural and technical
515 processes. Reviews in Mineralogy and Geochemistry, 73, 513-578.
- 516 Simon, G., Kesler, S.E. and Chryssoulis, S. (1999) Geochemistry and textures of gold-bearing
517 arsenian pyrite, Twin Creeks, Nevada: Implications for deposition of gold in Carlin-type
518 deposits. Economic Geology, 94, 405-422.
- 519 Spiridonov, E. and Yanakieva, D. (2009) Modern mineralogy of gold: overview and new data,
520 Archeosciences, 33, 67–73 (in Russian).
- 521 Symonds, R.B., Rose, W.I., Gerlach, T.M., Briggs, P.H. and Harmon, R.S. (1990) The
522 evaluation of gases, condensates, and SO₂ emissions from Augustine Volcano, Alaska:
523 the degassing of a Cl-rich volcanic system. Bulletin of volcanology, 52, 355–374.
- 524 Taran, Yu.A., Bernard, A., Gavilanes, J.C. and Africano, F. (2000) Native gold in mineral
525 precipitates from high-temperature volcanic gases of Colima volcano. Mexico. Applied
526 Geochemistry, 15, 337–346.
- 527 Vergasova, L.P., Starova, G.L., Serafimova, E.K., Filatov, S.K., Filosofova, T.M. and Dunin-
528 Barkovskii, R.L. (2000). Native gold of volcanic exhalations in the slag cones of the huge
529 Fractured Tolbachinskii eruption. Vulkanologiya i Seismologiya, 5, 19–27 (in Russian).
- 530 Warmada, W., Lehmann, B. and Simandjuntak, M. (2003) Poly-metallic sulfides and sulfosalts
531 of the Pongkor epithermal gold-silver deposit, West Java, Indonesia. Canadian
532 Mineralogist, 41, 185–200.
- 533 White, J.L., Orr, R.L. and Hultgren, R. (1957) Thermodynamic properties of silver–gold alloys.
534 Acta Metallurgica, 5, 747–760.
- 535 Yang, S., Blum, N., Rahders, E. and Zhang Z. (1998) The nature of invisible gold in sulfides
536 from the Xiangxi Au-Sb-W ore deposit in northwestern Hunan, People's Republic of
537 China. The Canadian Mineralogist, 36, 1361-1372.
- 538 Yushko-Zakharova, O.E., Ivanov, V.V., Soboleva, L.N., Shcherbachev, D.K., Kulichikhin, R.D.,
539 Timofeeva, O.S. and Dubakina, L.S. (1986) Minerals of noble metals, Moscow: Nedra (in
540 Russian).
- 541 Zevin, D.Yu., Migdisov, A.A. and Williams-Jones, A.E. (2007) The solubility of gold in
542 hydrogen sulfide gas: an experimental study. Geochimica et Cosmochimica Acta, 71,
543 3070–3081.
- 544 Zhen-jie, C., Yong-fen, G., Ji-liang, Z., Wen-yuan, X. and Feng-ge, W. (1979) On discovery and
545 investigation of liujinyinite. Kexue Tongbao, 24, 843–848.

546

547 **Figure captions:**

548 **Figure 1.** X-ray diffraction pattern showing that the Au-Ag sulfide from Khopto (1) is
549 petrovskaita (2) (sheet № 19-1146). Some weak peaks in the diffraction pattern belong to
550 uytenbogaardtite (3) (sheet № 33-0587) and gold (4) (sheet № 04-0784).

551 **Figure 2.** A rim of petrovskaita after native gold at the Khopto deposit (Tyva, Russia): a –
552 reflected light; b – BSE image; c, d – representative ED spectra of the minerals in listed points
553 shown in b; e-g - X-ray images $AgL\alpha$ (e), $AuL\alpha$ (f) and $SK\alpha$ (g).

554 **Figure 3.** A rim of Au-Ag sulfide after native gold (820 ‰) with an intermediate micro rim of
555 higher fineness gold (920 ‰) at the contact: a – BSE image; c-f – representative ED spectra of
556 the minerals in listed points shown in a; d - graphs of EDS results (1-13 points) across native
557 gold and Au-Ag sulfides grains showing variations in the proportions of Au, Ag and S. In photo
558 a: 1–28 are the points of measurement of mineral composition.

559 **Figure 4.** Native gold and Au-Ag sulfides (acanthite, uytenbogaardtite) filling a fracture in
560 quartz at the Ulakhan deposit: a - reflected light; b - BSE image; c, d – details of the previous
561 photo showing native gold grains with a Au-Ag sulfides rim and intermediate veinlets (c) and
562 microrim (d) of higher fineness gold (white).

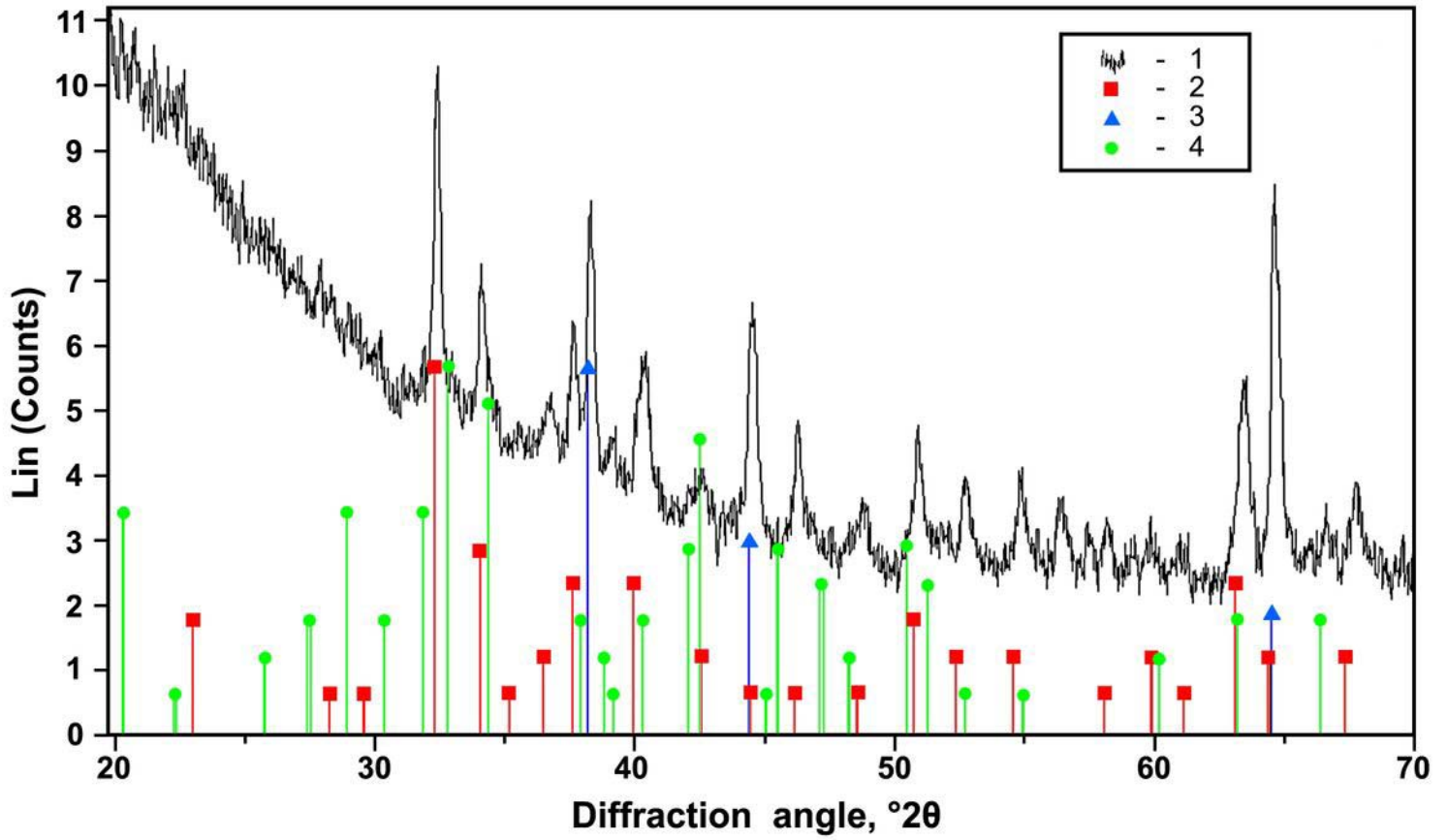
563 **Figure 5.** Rim of petrovskaita after native gold at Yakutskoe deposit (Russia): a – reflected light;
564 b – BSE image; c - BSE image fragment of grain in b (outlined by a line); d - graphs of EDS
565 results (1-10 points on c) across native gold and petrovskaita grains showing variations in the
566 proportions of Au, Ag and S.

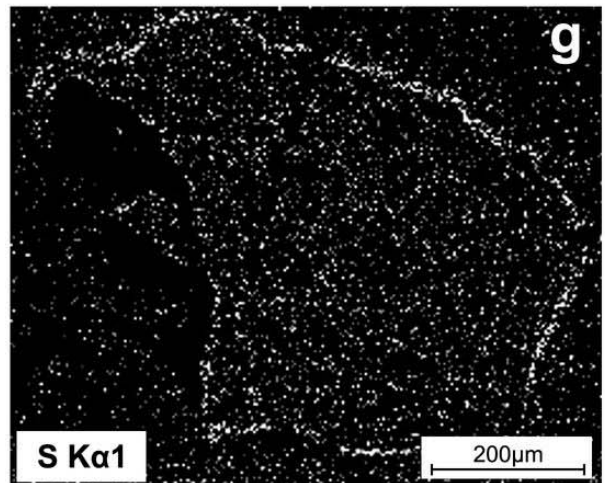
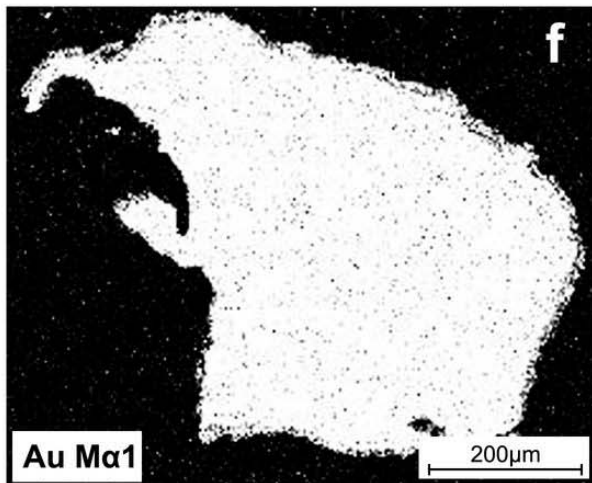
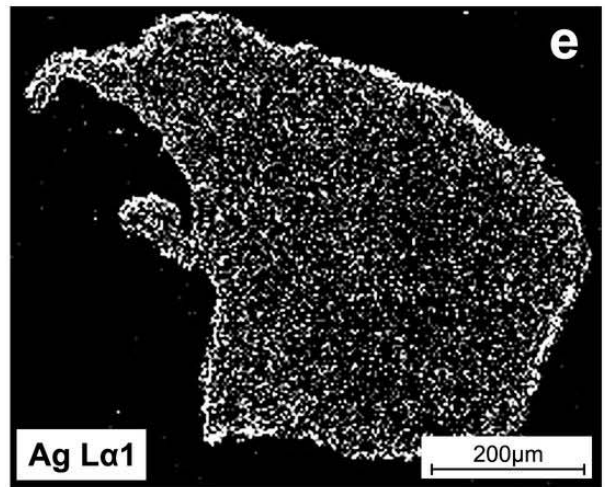
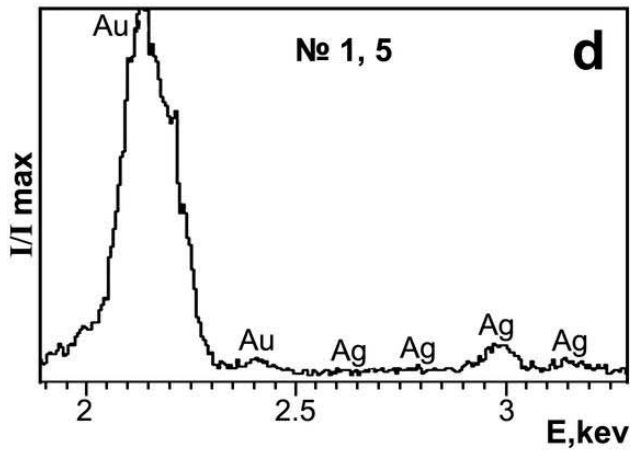
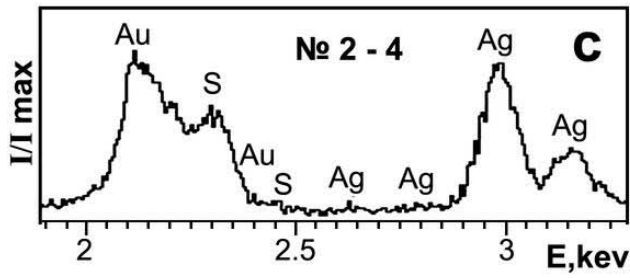
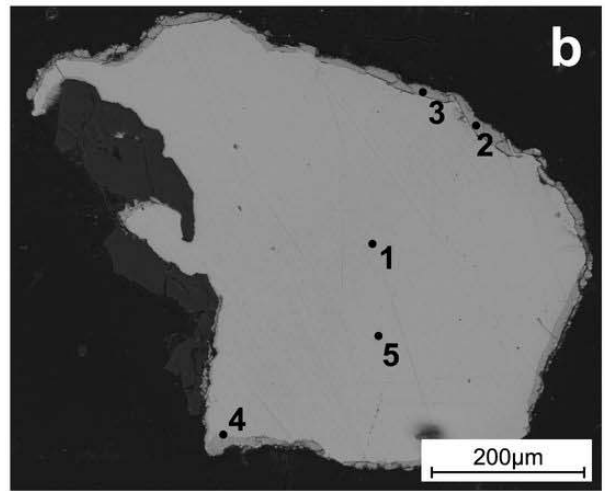
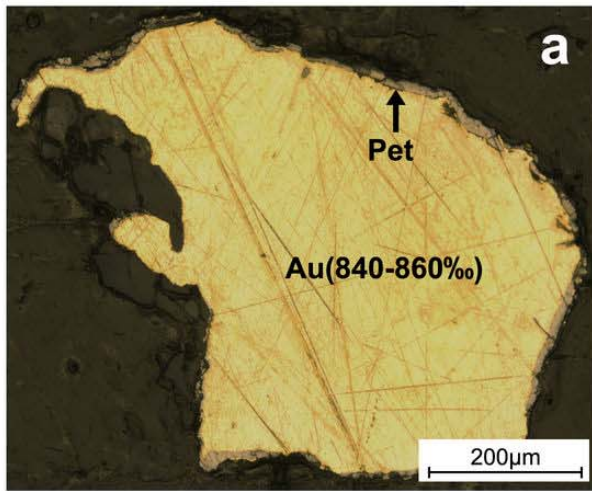
567 **Figure 6.** The compositions (in mole fraction) of native gold and associated Au-Ag sulfide rims
568 from the Khopto (a), Ulakhan (b) and Yakutskoe (c) deposits.

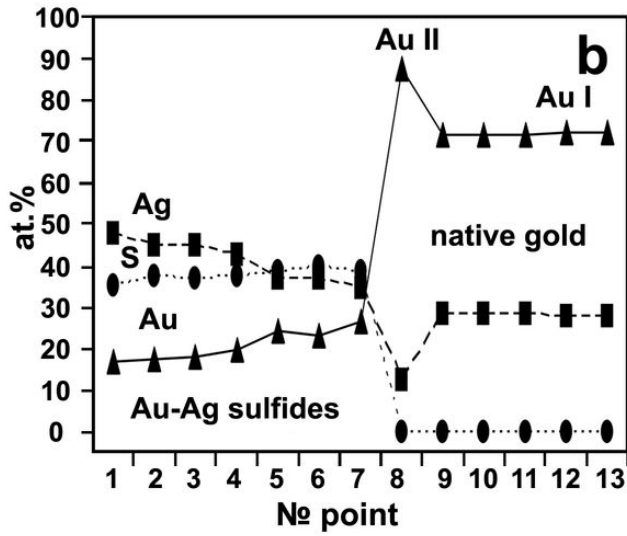
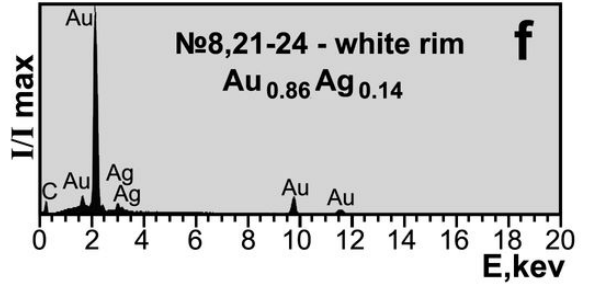
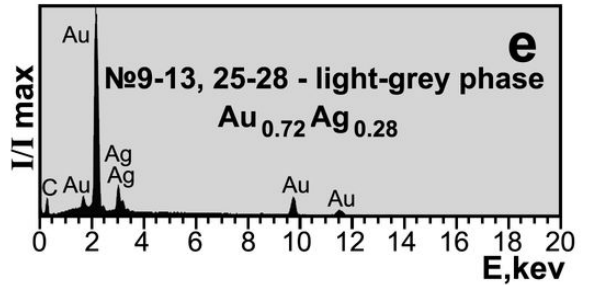
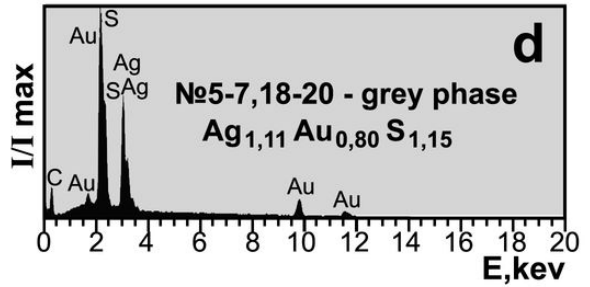
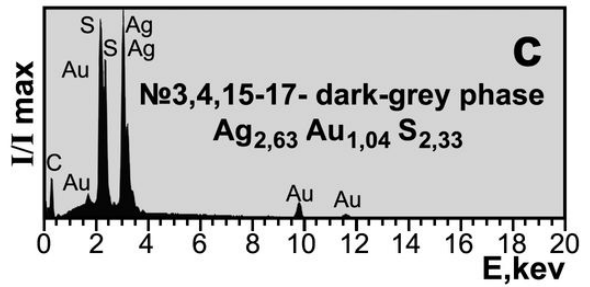
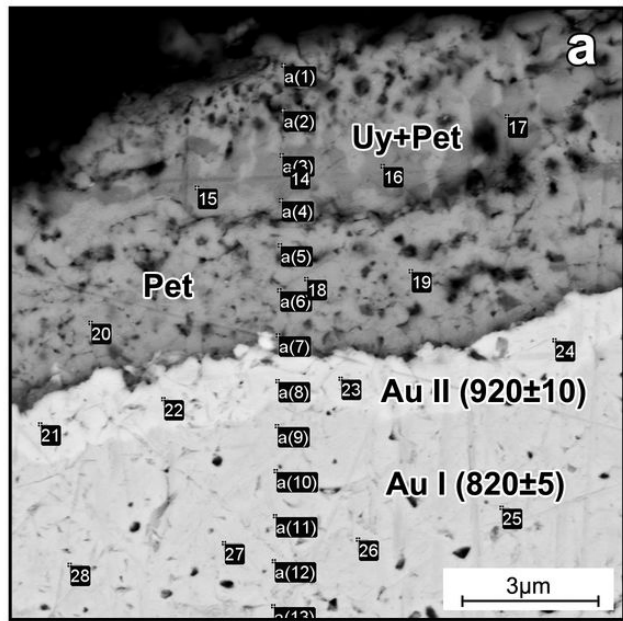
569 **Figure 7.** Overview of the proposed sulfidation reactions of native gold: a - with the formation
570 of two Au-Ag sulfides, b – with formation of one of Au-Ag sulfides - Ag_2S , Ag_3AuS_2 or $AgAuS$
571 and higher fineness or pure gold. Numbers of reactions 2-10 correspond to numbering in the text.

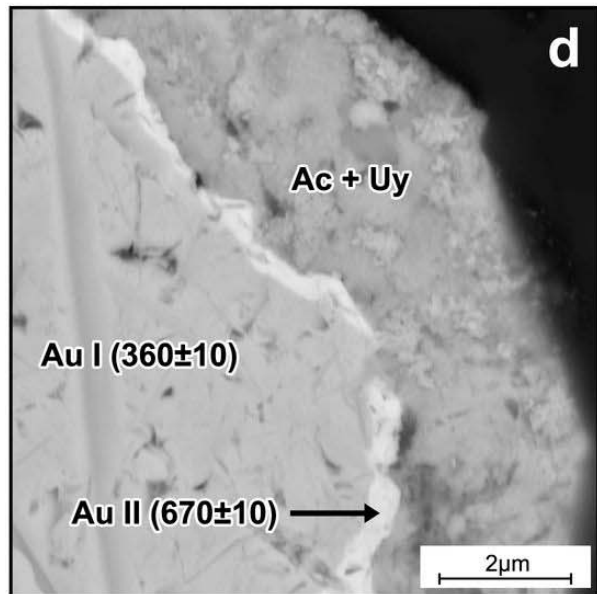
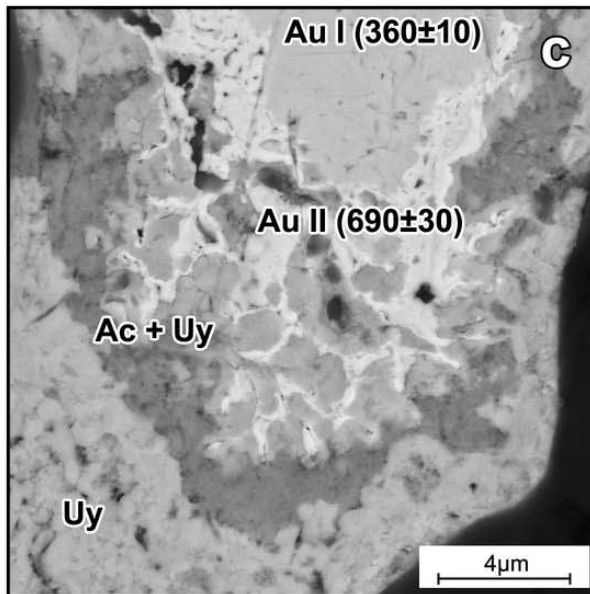
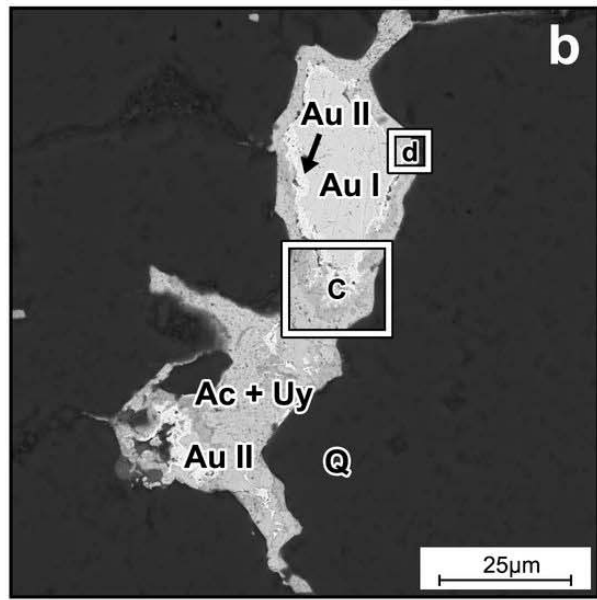
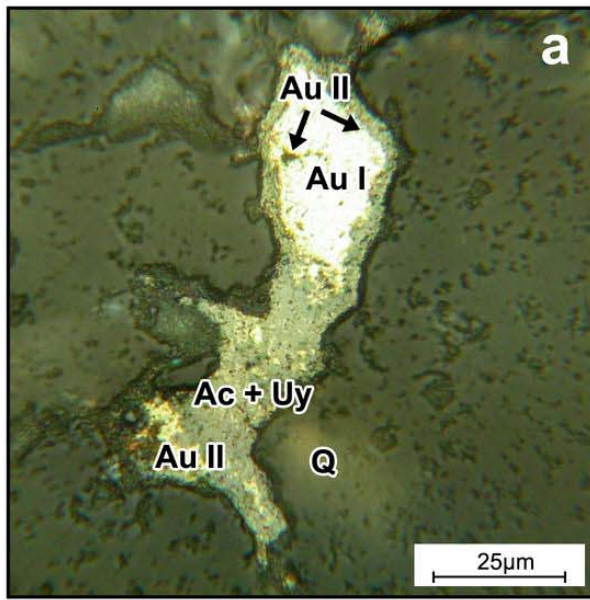
572 **Figure 8.** Microcrystals of uytenbogaardtite on the dark surface of native gold (a) and porous
573 structure of native gold nearby Au-Ag sulfide (b). Dorozhnoe deposit.

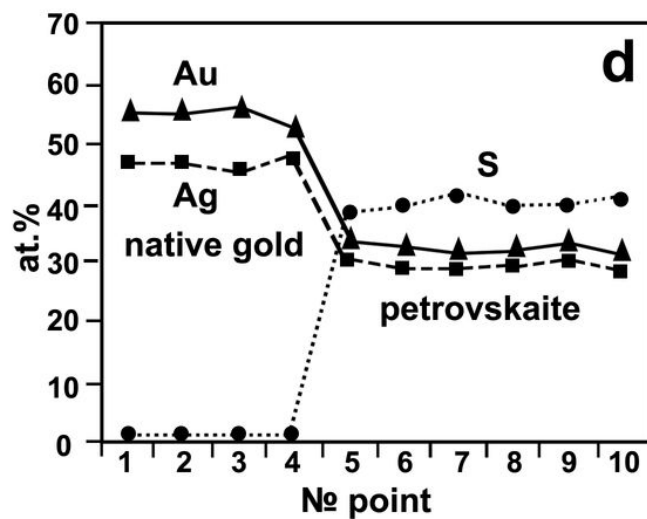
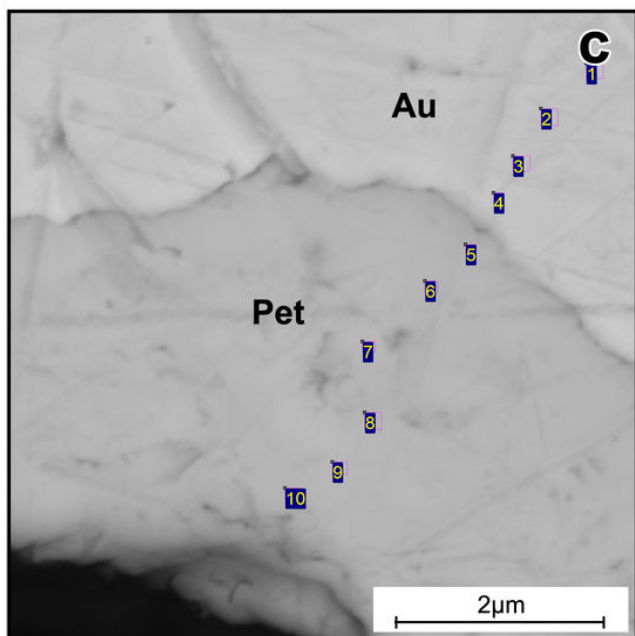
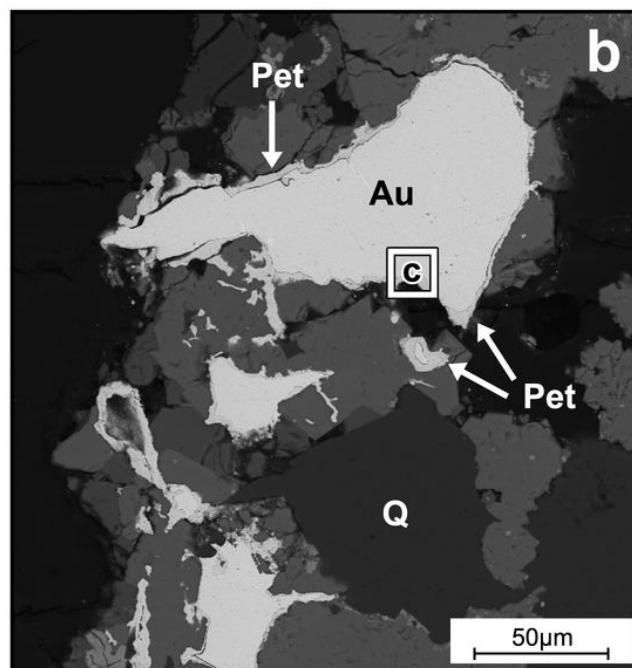
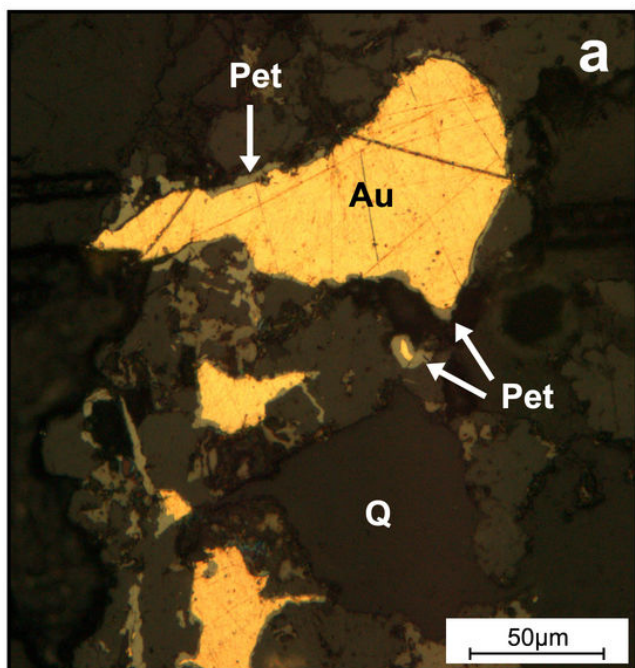
574

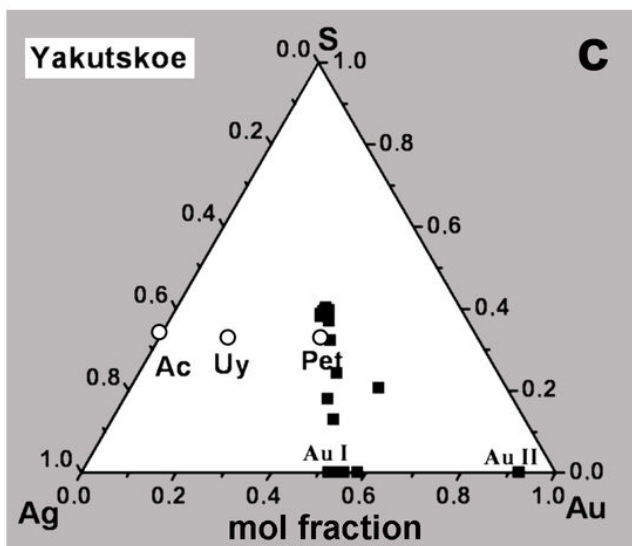
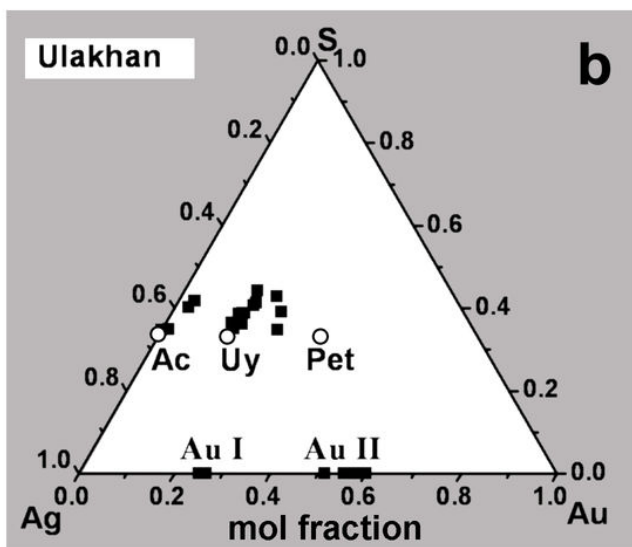
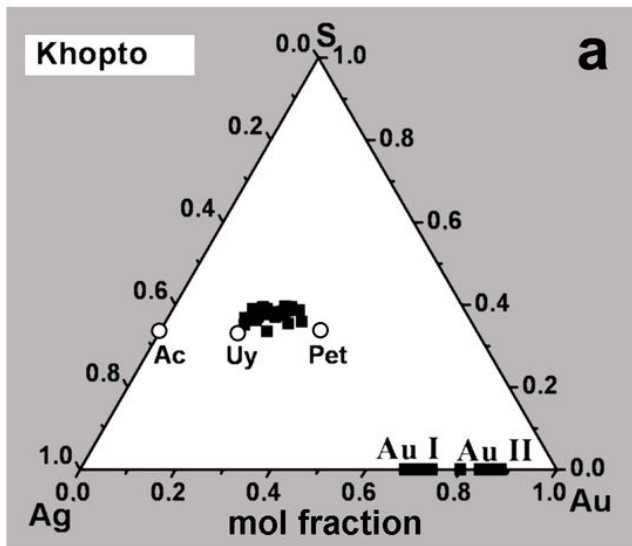


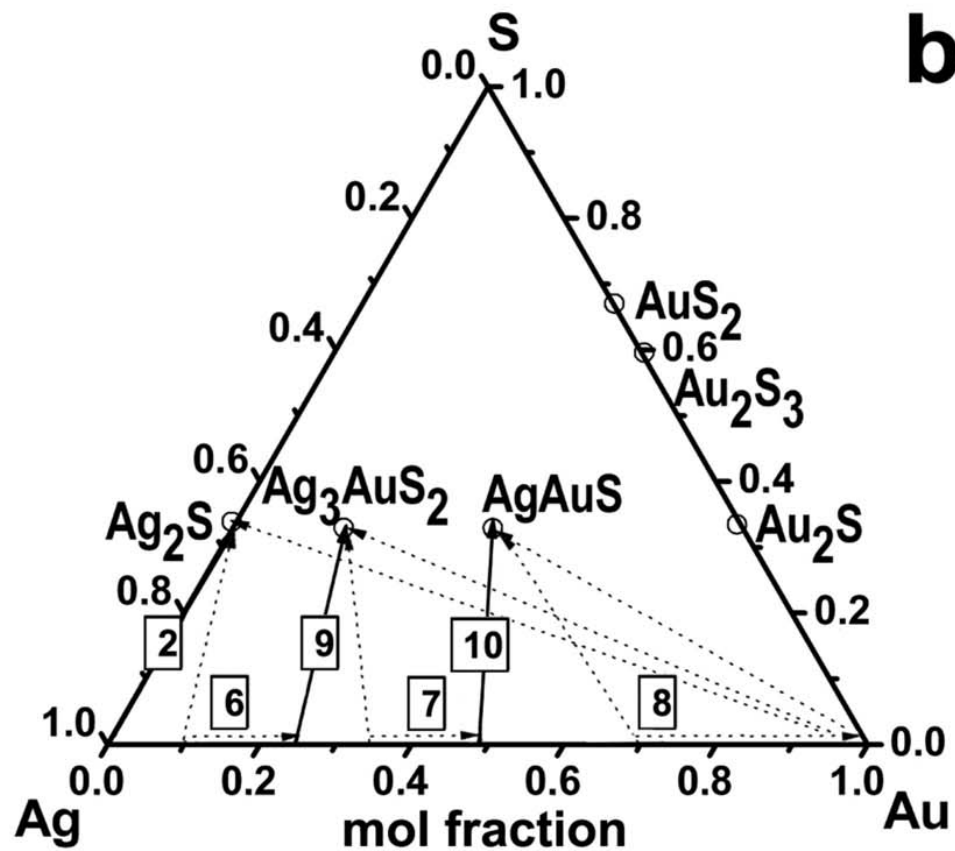
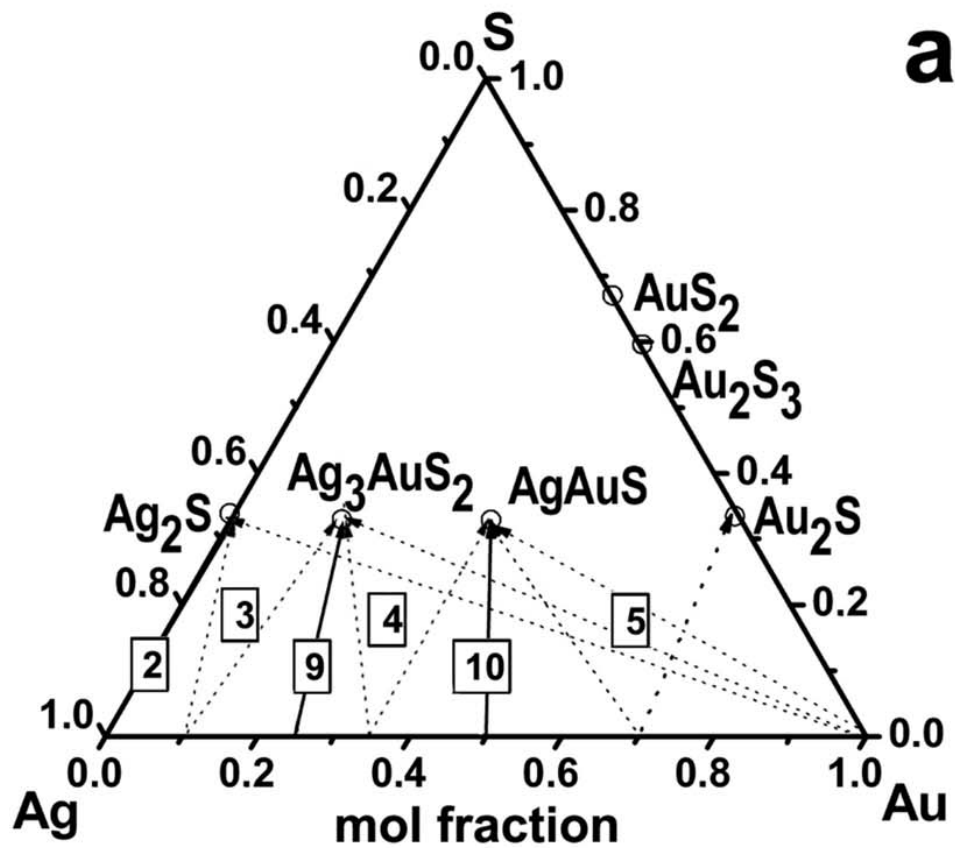












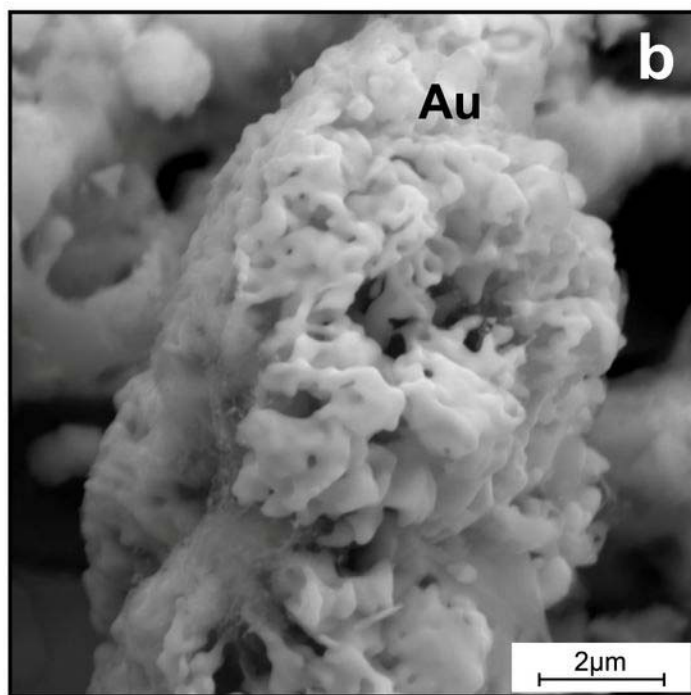
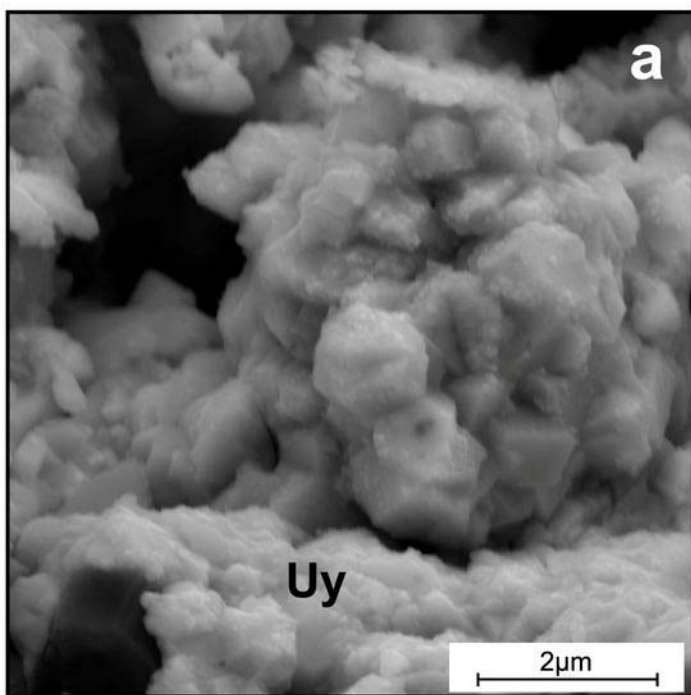


Table 1. Representative electron microprobe analyses of Au-Ag sulfides (in wt %)

Deposits	n	Au	Ag	S	minerals	References
Khopoto	30	40.46÷48.56	40.38÷46.82	11.06÷12.72	Uy+Pet	this paper
	6	34.01÷44.00	43.44÷56.74	10.08÷11.53	Uy	Gas'kov et al. 2006
	37	47.21÷51.13	36.22÷41.11	11.99÷13.04	Pet	this paper
	43	36.52 ÷ 39.88	46.55÷50.23	12.24÷13.22	Uy	- " -
Ulakhan	7	30.95÷29.72	57.15-58.65	11.90-12.75	Uy	this paper
	5	0	84.29÷85.88	13.49÷13.76	Ac	- " -
Yakutskoe	24	58.48÷59.18	29.19÷29.93	11.31÷12.29	Pet	this paper
	4	56.1÷60.8	29÷35.3	7.3÷7.9	Pet	Nekrasov et al. 1988
	10	39.4÷51.8	36÷44	6.8÷7.4	Pet	Samusikov et al. 2002
Dorozhnoe	7	30.55÷35.18	54.18÷57.91	10.46÷10.98	Uy	this paper
	11	49.68÷56.71	33.96÷42.15	7.78÷8.82	Pet	- " -
	3	48.1÷55.6	33.3÷40.9	8.3÷10.1	Pet	Al'shevskii 2001
Konechnoe	6	30.53÷33.87	44.6÷52.74	12.21÷14.5	Uy	Proskurnin et al 2010
Yunoe	15	23.40÷26.10	64.80÷66.90	8.50÷9.00	Uy	Pal'yanova and Savva
	8	0	84.10÷85.00	14.20÷14.80	Ac	2009; this paper
Ideal composition		33.69	55.35	10.97	Uy	Ag ₃ AuS ₂
		58.46	32.02	9.52	Pet	AgAuS
		0	87.06	12.94	Ac	Ag ₂ S
		92.47	0	7.53	-	Au ₂ S

n - number of analyses, Ac – acanthite, Uy – uytenbogaardtite, Pet – petrovskaite.

Table 2. Types of textural relationships between native gold (silver) and acanthite, uyttenbogaardtite and petrovskaita at some gold deposits, the fineness of primary and secondary native gold at the contact with Au-Ag sulfides.

Deposits, ore occurrences	Boundaries		fineness, ‰		References
			I	II	
Nazareno	Ac / Ag	Type 1	0	no	Greffie et al. 2002
Kubaka	- « -	- « -	0-100	no	Savva 1995
Comstock	Ac / Au	- « -	250	no	Barton et al. 1978
Konechnoe	Uy / Au	- « -	350-520	no	Proskurnin et al. 2011
Yakutskoe	Pet / Au	- « -	630-670	no	Nekrasov et al. 1988
- « -	- « -	- « -	650-680	- « -	this paper
Maikain	- « -	- « -	650-999	no	Nesterenko et al. 1984
Broken Hills	- « -	- « -	620-670	no	Cocker et al. 2013
Tambang Sawah	Ac + Uy / Au	Type 2	570	no	Barton et al. 1978
Kupol	- « -	- « -	590-690	no	Savva et al. 2012
Kubaka	- « -	- « -	600-700	no	Savva 1995
Yunoe	- « -	- « -	560-700	no	this paper
Rabenstein	- « -	- « -	360-610	no	Majzlan 2009
Broken Hills	- « -	- « -	560-670	no	Cocker et al. 2013
Dorozhnoe	Uy+Pet/Au	- « -	680-800	no	this paper
Krutoe	- « -	- « -	870-880	no	Savva et al. 2010
Lac Bullfrog	Uy/Au II/Au I	Type 3	650-680	840	Castor and Sjoberg 1993
Original Bullfrog	- « -	- « -	570-670	870	- « -
Nazareno	- « -	- « -	560-740	700-800	Greffie et al. 2002
Broken Hills	- « -	- « -	560-740	820-900	Cocker et al. 2013
Morning Star	Ac+Uy/Au II/Au I	Type 4	610-720	780-930	Sheets et al. 1995
Nazareno	- « -	- « -	560-740	700-800	Greffie et al. 2002
Cirotan	- « -	- « -	320-760	780-930	Marcoux et al. 1993
Ulakhan	- « -	- « -	200-390	750-850	Savva and Pal'yanova 2007
- « -	- « -	- « -	350-390	660-720	this paper
Broken Hills	- « -	- « -	560-570	620-640	Cocker et al. 2013
Khopto	Uy+Pet/Au II/Au I	- « -	820±5	920±10	this paper
Comstock	Ac/Uy/Au II/Au I	Type 5	450	600	Barton et al. 1978
Pongkor	Ac/Uy /Au II/Au I	- « -	420-700	700-800	Greffie et al. 2002

Legend: Au I - early generation of native gold, Au II – later generation of native gold (in microrims between Au-Ag sulfides and native gold I), Ag – native silver.